



UNIVERSIDADE ESTADUAL DE CAMPINAS
SISTEMA DE BIBLIOTECAS DA UNICAMP
REPOSITÓRIO DA PRODUÇÃO CIENTÍFICA E INTELLECTUAL DA UNICAMP

Versão do arquivo anexado / Version of attached file:

Versão do Editor / Published Version

Mais informações no site da editora / Further information on publisher's website:

<https://onlinelibrary.wiley.com/doi/full/10.1002/tcr.201700086>

DOI: 10.1002/tcr.201700086

Direitos autorais / Publisher's copyright statement:

©2018 by Wiley. All rights reserved.

DIRETORIA DE TRATAMENTO DA INFORMAÇÃO

Cidade Universitária Zeferino Vaz Barão Geraldo

CEP 13083-970 – Campinas SP

Fone: (19) 3521-6493

<http://www.repositorio.unicamp.br>

Nano Silver Vanadate AgVO_3 : Synthesis, New Functionalities and Applications

Ana Paula de Melo Monteiro,* Raphael Dias Holtz, Leandro Carneiro Fonseca, Carlos Henrique Zanini Martins, Marcelo de Sousa, Luis Augusto Visani de Luna, Djalma Lucas de Sousa Maia, and Oswaldo Luiz Alves*^[a]

Abstract: Silver vanadates have been widely investigated because of their many interesting properties and their potential use in several applications. In addition to this, a large number of groups have investigated silver vanadates in the form of nanostructures. Here, we address first the synthesis and properties of nanosilver vanadate. Different techniques, such as precipitation, thermal decomposition, hydrothermal treatment, and sol-gel, are among the methods that have been employed for the controlled synthesis of silver vanadate. The use of nanosilver vanadate for the development of novel electronic devices, catalysts, and antibacterial agents for industry and biomedical applications will then be discussed. In this sense, the present review highlights the major advances regarding the synthesis, properties and applications of nanostructured silver vanadates.

Keywords: Nanostructured silver vanadate, nanomaterials, synthesis, properties, applications

1. Introduction

Silver vanadate nanostructures hold a special place in the broad field of nanotechnology. The advances in this particular area have shown that the limitations of bulk materials can be overcome by size reduction. This is particularly appealing when applied to a material such as silver vanadate, as it opens up the possibility of extending and improving device functionalities and even using silver vanadate in applications previously considered inaccessible with this material. In this review, we will focus on the recent advances in the synthesis of silver vanadate nanostructured materials, with special emphasis on understanding their properties and the correlated applications. Silver vanadates (AgVO_3 , $\text{Ag}_2\text{V}_4\text{O}_{11}$, Ag_3VO_4 ,

$\text{Ag}_4\text{V}_2\text{O}_7$, etc.) are very important due to their specific photoelectronic and chemical properties.^[1] To date, $\text{Ag}_2\text{V}_4\text{O}_{11}$, Ag_3VO_4 and $\text{Ag}_4\text{V}_2\text{O}_7$ have been extensively studied, especially as a battery cathode material with high discharge capacity. Their high rate capability and long-term reliability are important for advanced medical implantable devices such as cardioverter defibrillators, neurostimulators, atrial defibrillators, and drug infusion devices.^[2,3] Therefore, in this review, we will focus only on the silver vanadates β - AgVO_3 and α - AgVO_3 .

2. Crystal Structures and Properties of Alfa and Beta AgVO_3

Four crystal structures of AgVO_3 , i.e., three metastable α -type, Y-type, and δ -type and thermodynamically stable β -type, have been reported in the literature.^[4] The crystal structures of lambda and gamma compounds are known and were determined by powder X-ray diffraction. However, their crystal structures have not been obtained.

The structure of β - AgVO_3 was determined using single-crystal X-ray diffraction and compared to the reported

[a] A. P. de Melo Monteiro, R. Dias Holtz, L. Carneiro Fonseca, C. H. Zanini Martins, M. de Sousa, L. A. V. de Luna, D. L. de Sousa Maia, O. L. Alves
Laboratory of Solid State Chemistry (LQES) and NanoBioss Laboratory,
Institute of Chemistry
University of Campinas
P.O. Box 6154, Campinas, Sao Paulo 13083-970, Brazil
E-mail: apdemmm@gmail.com
oalves@iqm.unicamp.br

structures of $\text{Ag}_2\text{V}_4\text{O}_{11}$ and $\delta\text{-Ag}_x\text{V}_2\text{O}_5$.^[5] $\beta\text{-AgVO}_3$ powder was prepared by heating a 1 : 1 mixture of Ag_2O and V_2O_5 in a gold crucible at 420°C for 12 h under a stream of oxygen gas. The mixture was reheated under the same conditions in order to obtain a well crystallized red powder. To form single crystals, the $\beta\text{-AgVO}_3$ powder was heated in a gold crucible under an oxygen atmosphere at 500°C for 10 h, cooled to 450°C at a rate of 2°C h^{-1} , and then quenched to room temperature. The $\beta\text{-AgVO}_3$ crystal was assigned to a monoclinic system with space group Cm , and the structure consisted of infinite $[\text{V}_4\text{O}_{12}]_n$ chains of edge-shared VO_6 octahedra where the chains were *zigzag* in shape. The VO_6 octahedra were distorted, with four different V–O bond lengths ranging from 1.67(4) to 2.44(8) Å. The four silver atoms were distributed in three types of surroundings: the first Ag atom was six coordinated with the bonded oxygen atoms positioned in a weakly distorted octahedron (typical bond distance = 2.43(4) Å); the second and third Ag atoms were five coordinated, with the bonded oxygen atoms positioned in a square pyramid, where the Ag–O bonds were similar in magnitude (typical bond distance = 2.40 Å); and the fourth Ag atom was seven coordinated, with the bonded oxygen atoms positioned in a monocapped trigonal prism, where the Ag–O bond lengths ranged from 2.22 to 2.89 Å. Since the fourth Ag atom was positioned in the largest site and the monocapped trigonal prisms shared faces along the [010] direction, the authors proposed that these Ag atoms might be particularly mobile within the crystalline lattice. Finally, due to the strong three dimensional network of V_4O_{16} double chains held together by Ag_1O_6 octahedra and further interlinked by Ag_2O_5 and Ag_3O_5 square pyramids, the authors proposed that $\beta\text{-AgVO}_3$ can be envisioned structurally as $\text{Ag}[\text{Ag}_3\text{V}_4\text{O}_{12}]$, where Ag^+ is the fourth silver cation. The authors also discussed the structural similarities among $\beta\text{-AgVO}_3$, $\text{Ag}_2\text{V}_4\text{O}_{11}$, and $\delta\text{-Ag}_x\text{V}_4\text{O}_{10}$ and proposed possible routes of interconversion via the loss of Ag_2O or O.^[5]

Table 1 shows some properties such as the crystal structure, band gap energy and density of $\beta\text{-AgVO}_3$ and $\alpha\text{-AgVO}_3$. Between the phases $\beta\text{-AgVO}_3$ and $\alpha\text{-AgVO}_3$, the vanadium atoms are tetracoordinated by oxygen atoms and pentacoordinated by oxygen, respectively.^[6] The $\alpha\text{-AgVO}_3$ structure is composed of tetrahedrons of VO_4 arranged in space forming *zigzag* chains in which the corner oxygen is shared between the sheets of octahedrons with silver atoms in

the center, which is different from that of $\beta\text{-AgVO}_3$, in which the vanadium atoms are in the center of the octahedrons, Figure 1.^[7] The distinctive properties of silver vanadate could be ascribed to the diversity of the assembled geometries of V, O, and Ag elements.

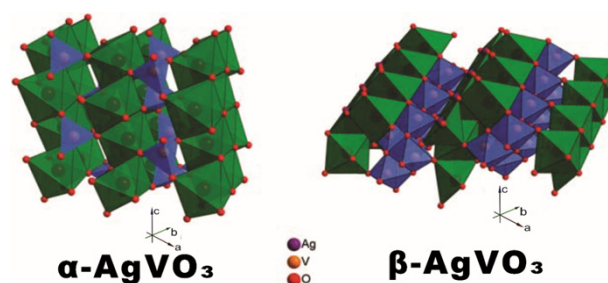


Figure 1. Crystal structure of the $\alpha\text{-AgVO}_3$ and $\beta\text{-AgVO}_3$. Adapted from ref. [9].

The hybridization of V 3d orbitals and Ag 5s orbitals constitutes the conduction band of silver vanadate, and the valence band of silver vanadate is associated with O 2p orbitals hybridized with Ag 3d orbitals, yielding a narrow band gap and highly dispersed conduction band and valence band.^[10] The properties of silver vanadate are highly dependent on its composition, morphology, crystal structure and surface properties. These parameters greatly affect the photocatalytic and antibacterial activities, such as electrochemical, sensing, optical and electrical properties. The crystal structure and composition of such materials are strongly influenced by the reaction conditions employed and intensively affect their functionalities.^[8] Therefore, several approaches have been developed for the synthesis of silver vanadate materials to explore these physicochemical properties. Initially, AgVO_3 was prepared by heating the metal oxides Ag_2O and V_2O_5 .^[11] After that, several other methods, such as precipitation, sol–gel, ion exchange, hydrothermal treatment, ultrasonic irradiation and biomineralization, were also reported.^[12] Silver vanadates AgVO_3 synthesized using these approaches as reported in the literature will be discussed along with their potential use in a variety of applications.

3. Synthesis

Silver vanadates display a variety of both stoichiometric and nonstoichiometric phases. Thus, variations in reaction conditions, starting materials, concentration of the initial reagents and reagent stoichiometry for the preparation of silver vanadates result in a range of products that display different structures and properties. In addition, this synthetic param-

Table 1. Properties of the $\alpha\text{-AgVO}_3$ and $\beta\text{-AgVO}_3$.

Phase	Density (g cm^{-3})	Band gap (eV)	Spatial group	Ref.
$\alpha\text{-AgVO}_3$	4.81	2.50	C2/c	4
$\beta\text{-AgVO}_3$	5.32	2.01	C12m1	8

Table 2. Crystal nanostructures, reagents and methods used in the synthesis of the AgVO₃.

Phases	Reagent	Method	Ref.
Nanorods AgVO ₃	Ag pellets, Vanadium target	Pulsed laser deposition/thermal evaporation	[6]
Nanowires β-AgVO ₃	AgNO ₃ , NH ₄ VO ₃ , H ₂ O, acetic acid (C ₂ H ₄ O ₂)	Hydrothermal	[19]
Microstar grains α-AgVO ₃	AgNO ₃ , NH ₄ VO ₃ , H ₂ O, n-heptane surfactant (Triton X-100), co-surfactant (1-hexanol),	Microemulsion Coprecipitation	[20]
Nanowires α-AgVO ₃	AgNO ₃ , NH ₄ VO ₃ , H ₂ O, bovineserum albumin (BSA), bovinehemoglobin (BHb), lysozyme (Lyz)	Biom mineralization	[21]
Nanorods AgVO ₃	AgNO ₃ , NH ₄ VO ₃ , H ₂ O, H ₂ O ₂	Coprecipitation/thermal decomposition	[22]
Nanorods β-AgVO ₃	AgNO ₃ , NH ₄ VO ₃ , H ₂ O	Hydrothermal/ultrasound/microwave assistance	[23]
Nanorods β-AgVO ₃	AgNO ₃ , NH ₄ VO ₃ , H ₂ O, 1-dodecanol	Thermal decomposition	[24]
Micro-rods β-AgVO ₃	V ₂ O ₅ , AgNO ₃ , citric acid (C ₆ H ₈ O ₇ ·H ₂ O), malic acid (C ₄ H ₆ O ₅), tartaric acid (C ₄ H ₆ O ₆)	Sol-gel/thermal decomposition	[25]
Nanobelts β-AgVO ₃	AgNO ₃ , NH ₄ VO ₃ , H ₂ O, HNO ₃ , hexadecyl trimethyl ammonium bromide (CTBA)	Hydrothermal	[26]
Nano needle-like β-AgVO ₃	V ₂ O ₅ gel, Ag ₂ O powder	Sol-gel/Ultrasonic treatment	[27]
Nanorods β-AgVO ₃	Silver salicylate (Ag(HSal)), NH ₄ VO ₃ , Organic solvent, Surfactant	Ultrasonic irradiation	[28]
Nanowires β-AgVO ₃	AgNO ₃ , NH ₄ VO ₃ , H ₂ O	Ultrasonic radiation	[29]
Nano-ribbons β-AgVO ₃ /V _{1.6}	AgNO ₃ , NaVO ₃ , H ₂ O, HNO ₃	Sol-gel	[30]
Nanorods α-AgVO ₃	AgNO ₃ , NH ₄ VO ₃ , H ₂ O	Coprecipitation	[31]
Nanowires 3D β-AgVO ₃	AgNO ₃ , NH ₄ VO ₃ , H ₂ O, acetonitrile	Hydrothermal	[32]
Nanowires β-AgVO ₃	(tin-doped indium oxide) conductive substrate, AgNO ₃ , V ₂ O ₅ , H ₂ O, LiF	Hydrothermal	[33]
Nanowires β-AgVO ₃	AgNO ₃ , NH ₄ VO ₃ , H ₂ O	Hydrothermal	[34]
Nanoribbons β-AgVO ₃	AgNO ₃ , V ₂ O ₅ , H ₂ O, pyridine	Hydrothermal	[35]
Microribbons β-AgVO ₃	AgNO ₃ , NH ₄ VO ₃ , H ₂ O, pyridine	Hydrothermal	[36]

ters control allows the tuning of the crystallization process towards the sample nano-structuration.

The nanostructures, reagents and methods are shown in Table 2. Various AgVO₃ nanostructures (nanorods, nanobelts, nanoribbons and nanowires) were synthesized by chemical, hydrothermal, and hydrothermal-assisted methods and a combination of methods.

The historical evolution of silver vanadate chemistry in terms of the variety of synthetic strategies essential for specific phase preparation will be presented. Some of the earliest published works on silver vanadate were authored by Roscoe in 1871,^[12] Ditte in 1887^[13] and Browning and Palmer in 1910.^[14] In 1930, Britton and Robinson^[15] conducted electrochemical titrations of aqueous silver nitrate and sodium vanadate using silver electrodes. The same authors observed

that vanadates of silver with various Ag:V ratios and colors were formed as precipitates, with the 3:1 and 1:1 precipitates being orange and the 2:1 precipitate being light yellow. In addition, the solubility products of the vanadates were determined, ranging from 1×10^{-24} for the 3:1 compound to 2×10^{-14} for the 2:1 silver vanadate and 5×10^{-7} for the 1:1 compound.^[15] Subsequently, in 1933, Britton and Robinson reported some of the experimental details associated with the isolation of the stoichiometric solids AgVO₃, Ag₄V₂O₇, and Ag₃VO₄ by various precipitation methods from cold AgNO₃/alkali vanadate solutions. The importance of aging or boiling the aqueous reactant solutions in order to obtain stoichiometric solids was emphasized.^[16] These investigations were restricted almost entirely to their synthesis and

physicochemical analysis. Since then, the synthesis of silver vanadate has been reported by many groups.

Fleury et al. used thermal analysis of a $\text{Ag}_2\text{O}-\text{V}_2\text{O}_5$ system to construct a phase diagram from the combination of the two solid oxides in five distinct stoichiometric ratios: 1:7, 1:2, 1:1, 2:1, and 3:1. The first four compounds, i.e., $\text{AgV}_7\text{O}_{18}$, $\text{Ag}_2\text{V}_4\text{O}_{11}$, AgVO_3 , and $\text{Ag}_4\text{V}_2\text{O}_7$, displayed melting points that ranged from 732°C for $\text{AgV}_7\text{O}_{18}$ to 392°C for $\text{Ag}_4\text{V}_2\text{O}_7$, where the decrease in the melting point corresponded to an increase in the Ag:V ratio. The thermal analyses were conducted under flowing oxygen in order to avoid the *in situ* formation of nonstoichiometric bronzes.^[17]

Ion exchange synthesis of silver vanadates from organically templated layered vanadates was reported by Sharma et al.^[18] Briefly, $(\text{org})_x\text{V}_2\text{O}_5$ was synthesized with 1 M solution of AgNO_3 . The progress of the ion exchange reaction was monitored by the color change of the reaction medium from green to yellow. It was suggested from XRD (X-ray diffraction) data that the parent layered structure of $(\text{org})_x\text{V}_2\text{O}_5$ was destroyed after mixing with silver nitrate. A gradual evolution of a $\beta\text{-AgVO}_3$ phase after 36 to 48 h was observed. The resulting product was AgVO_3 nanorods covered with small spherical silver nanoparticles with diameters of 2 to 5 nm as observed by TEM.

Holtz et al.^[19] reported the synthesis of silver vanadate nanowires decorated with silver nanoparticles, which acted as an antibacterial agent. These materials were synthesized by hydrothermal treatment and the reaction of ammonium vanadate with silver nitrate. The silver vanadate nanowires had lengths on the order of microns and diameters of approximately 60 nm. The diameter distribution of silver nanoparticles decorated on the nanowires varied from 1 to 20 nm. The influence of the pH of the reaction medium on the chemical structure and morphology of silver vanadates was also studied, and the authors found that synthesis performed at pH 5.5–6.0 led to silver vanadate nanowires with a higher morphological yield. It was also observed that increasing the amount of silver nitrate during the synthesis of silver vanadate nanowires led to systems with a large silver content on the nanowire surface. Transmission electron microscopy images of P2 (Ag/V molar ratio equal to 2), P3 and P4 (Ag/V molar ratios equal to 1 and 2 but without the addition of acetic acid) samples are shown in Figure 2. The samples were composed of nanowires with a diameter of approximately 60 nm and a length on the order of micrometers. They were decorated with AgNPs, and the nanowires were bundled as shown in Figure 2(a). Sample P3 (Figures 2(d)–(f)) also showed a heterogeneous distribution of AgNPs on the nanowires with the formation of some nanoparticle clusters. A dark field image obtained for sample P4 (see Figure 2(i)) is shown. Metallic and crystalline silver nanoparticles presented sizes ranging from 1 to 20 nm.^[19]

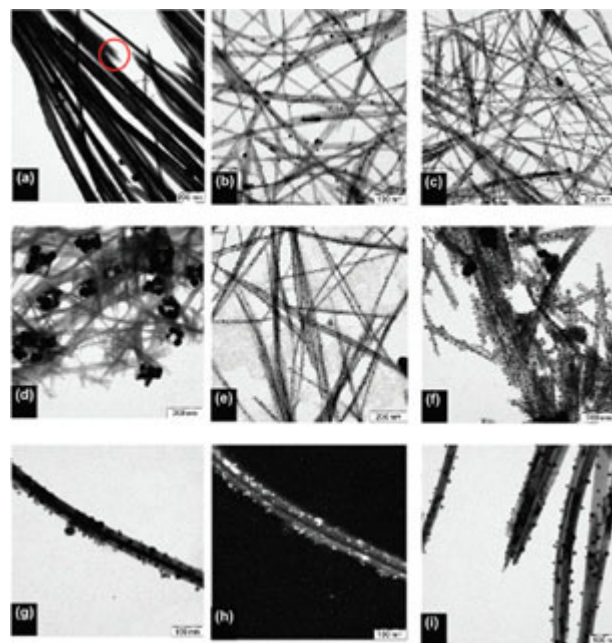


Figure 2. Transmission electron micrographs of silver vanadate nanostructures obtained by hydrothermal treatments ((a)–(c), (d)–(f), (g)–(i) stand for samples P2, P3 and P4, respectively). Images (a–g, i) and (h) were obtained in bright field, and dark field respectively. Adapted from ref. [19].

The microemulsion coprecipitation technique using low temperature to prepare silver vanadates was reported.^[20] Reverse micelles were formed by droplets of an aqueous solution encapsulated by a surfactant (Triton X-100) and a co-surfactant (1-hexanol), dispersed in n-heptane. For each silver vanadate (AgVO_3 and Ag_3VO_4) structure type, a microemulsion formed by a NH_4VO_3 aqueous solution was slowly added to another microemulsion with AgNO_3 salt, both in equal concentrations of 0.5 M. The characterization revealed the formation of both silver vanadates decorated with silver metallic nanoparticles on the surface.

Chen et al.^[21] presented a facile and bio-inspired route for the preparation of pure and highly crystalline metastable $\alpha\text{-AgVO}_3$. For this method, NH_4VO_3 (0.5 mmol) was dissolved into 10 mL of distilled water, and different amounts of protein (0–50 mg) were added. After that, a AgNO_3 solution (0.5 mmol, 10 mL) was added slowly under stirring. After stirring for 8 h at room temperature, the resulting precipitate was washed with distilled water and absolute ethanol several times. The precipitate was dried in a vacuum at 60°C for 6 h. Three kinds of proteins (bovine hemoglobin, bovine serum albumin, and lysozyme) were employed as an inducer, which had substantial effects on the nucleation and growth of $\alpha\text{-AgVO}_3$. The amount and surface charge of proteins had significant effects on the polymorphism and morphology of AgVO_3 . The $\text{VO}_3^-/\text{protein}$ complex provided a good control

on the crystallization rate, leading to the formation of a highly crystalline product. The average length of the micro-rods was 10 μm .^[21]

A facile, general and scalable strategy to prepare Ag nanoparticles anchored on silver vanadium oxides (SVOs), including AgVO_3 , $\text{Ag}_2\text{V}_4\text{O}_{11}$, $\text{Ag}_{0.33}\text{V}_2\text{O}_5$ and $\text{Ag}_{1.2}\text{V}_3\text{O}_8$, was developed.^[22] The preparation included the addition of NH_4VO_3 powder to a solution of H_2O_2 in deionized water, and after reaction, the authors observed the formation of a bright-yellow solution. This step was followed by the addition of a stoichiometric amount of AgNO_3 . The resulting homogeneous solution was dried to obtain solid precursors, which were further calcined in air at various temperatures to obtain vanadium oxides decorated with silver nanoparticles. Various silver vanadium oxides (AgVO_3 , $\text{Ag}_2\text{V}_4\text{O}_{11}$, $\text{Ag}_{0.33}\text{V}_2\text{O}_5$ and $\text{Ag}_{1.2}\text{V}_3\text{O}_8$) can be fabricated by tuning the ratio of V to Ag. The as-obtained Ag/SVO hybrids demonstrated highly improved electrochemical properties because of the enhanced electron conductivity. For example, the Ag/ AgVO_3 hybrid exhibited excellent rate capability: a high specific discharge capacity of 199 mAhg^{-1} can be reached at an ultra-high discharge current density of 5 Ag^{-1} .^[22]

Nanostructured silver vanadates synthesized by hydrothermal treatment assisted by ultrasound and microwave techniques were also reported.^[23] An amount of AgNO_3 was dissolved in distilled water and then added dropwise into a vessel containing NH_4VO_3 solution. The obtained mixture was vigorously stirred for 30 min and then ultrasonically treated for 30 min. The pH was adjusted to 6 and 7 by NH_4OH addition, and then, the solution was introduced into a Teflon-lined autoclave and hydrothermally treated by using microwave at 120 °C for 30 min. The obtained products were washed several times and dried at 80 °C overnight. Nanorods of silver vanadates with a diameter of 50–200 nm and a length of 0.5–2.0 μm were obtained. Interestingly, the silver vanadates showed a strong light absorbance in the visible light region at 470–500 nm. In comparison to TiO_2 nanoparticles, the silver vanadates exhibited much higher photocatalytic activity in the degradation of methylene blue under visible light irradiation. Moreover, these silver vanadates also exhibited high antibacterial activity, opening up their potential for environmental and biomedical applications.^[23]

Sivakumar et al.^[24] reported a facile approach to synthesize AgVO_3 nanorods using a thermal decomposition method. Ammonium metavanadate (0.1 mmol), silver nitrate (0.1 mmol) and 1 mL of 1-dodecanol were mixed, ground for 1 h in a mortar and then calcined at 450 °C for 5 h in a muffle furnace. An SEM (scanning electron microscopy) image of AgVO_3 prepared by calcination of the mixture of NH_3VO_4 and AgNO_3 at 450 °C for 5 h showed that the

synthesized sample was mostly rod-like particles with a highly crystalline structure. The length and width of the rods were several μm and 270 nm, respectively. Moreover, some irregularly shaped particles were also deposited on the surface of the rod-like particles.

The sol-gel method was employed to synthesize multi-scale AgVO_3 particles using citric acid, malic acid, and tartaric acid as reductants.^[25] First, 0.0066 mol vanadium pentoxide and 0.0198 mol citric acid ($\text{C}_6\text{H}_8\text{O}_7 \cdot \text{H}_2\text{O}$) were mixed and added to a beaker filled with 30 mL of distilled water under continuous stirring at 70 °C. After the suspension turned blue, 0.0132 mol silver nitrate was added to the solution and stirred for 30 min. Finally, the mixed solution was dried in an oven at 80 °C for 12 h. AgVO_3 particles were obtained by sintering the dried solid mixture at different temperatures for 3 h with a heating rate of 10 °C/min. The calcination products at 450 °C and 500 °C presented only monoclinic AgVO_3 , and the crystallinity of the samples increased as the temperature increased. These samples were characterized using SEM and showed mostly micro-sized rods that were 5–20 μm in length. In addition, there were nanoparticles with various sizes on the surface of the microrods.

A higher aspect ratio of AgVO_3 nanobelts fabricated via a hydrothermal route was proposed.^[26] In this context, the length of the nanobelts could be adjusted by modulating reaction parameters. Additionally, depending on the presence or absence of the surfactant hexadecyl trimethyl ammonium bromide (CTAB), straight or curled nanobelts were obtained, respectively. Silver nanoparticles, with a size of 5 and 10 nm, were produced uniformly on the surface of AgVO_3 nanobelts using α -aminopropionic acid as both a surface modifying and reducing agent. The formation of Ag nanoparticles created surface-enhanced Raman scattering (SERS) hot spots on the AgVO_3 nanobelts.

An ultrasonic irradiation method applied for the synthesis of silver vanadate was reported for the first time. This treatment accelerated the reaction between V_2O_5 gel and Ag_2O and reduced the time for reaction to approximately half an hour. Nanostructured AgVO_3 , $\text{Ag}_2\text{V}_4\text{O}_{11}$ and $\text{Ag}_{1.2}\text{V}_3\text{O}_8$ with different crystallinities were obtained.^[27]

Mohandes et al. reported that AgVO_3 micro/nanorods can be produced by using silver salicylate and ammonium metavanadate as starting reagents in the presence of ultrasound irradiation.^[28] SEM and XRD results indicated that AgVO_3 nanorods decorated with AgO nanoparticles were obtained in the presence of ethanol, cyclohexanol, DMSO and acetone. In addition, AgVO_3 nanorods with lower thicknesses were obtained by using DMF due to its lower vapor pressure. The obtained findings showed that by increasing the molecular weight of PEG, the dimensions of AgVO_3 nanorods decreased.

Ag/AgVO₃ nanowires and AgVO₃ nanorods were prepared in aqueous media via a facile sonochemical route.^[29] This method was based on acoustic cavitation, resulting in the continuous formation, growth and implosive collapse of bubbles in a liquid. An inert atmosphere promoted the deposition of Ag nanoparticles on the AgVO₃ nanowires.

The sol-gel method was used for the synthesis of AgVO₃/V_{1.6}⁵⁺V_{0.4}⁴⁺O₄ hydrogel/xerogel using immobilized dyes (methylene blue, crystal violet and iodide) for the reduction of silver nanoparticles onto the surface of vanadium oxide nanoribbons. In the synthesis conditions, the volume of nitric acid influenced the final composition of the hydrogel and its porous structure. The three dimensional reconstruction of a single nanoribbon demonstrated that the silver nanoparticles were anchored onto the silver vanadium oxide surface and that the widths of the nanoribbons could be as narrow as 5 nm.^[30]

α -AgVO₃ samples synthesized by a coprecipitation method at low temperatures were reported.^[7] Initially, 1 mmol NH₄VO₃ and 1 mmol AgNO₃ were individually melted in 35 mL of water under agitation at 30 °C. The solutions were mixed, and rapid materialization of α -AgVO₃ (yellow coloration) occurred. Coprecipitation was performed at 10, 20, and 30 °C. The powders were washed with distilled water and dried in an oven at 60 °C for 12 h. The crystallization of α -AgVO₃ was influenced by the solvent (H₂O), precursors (NH₄⁺ and NO₃⁻), and temperature involved in the reaction. The initial clusters formed in the solution (VO₃⁻_{aq} and Ag(NH₃)₂²⁺_{aq}) produced the building blocks for the early stages of the nucleation process; these, in turn, may become nano- or microparticles (amorphous, crystalline, and semi-crystalline). Water, NO₃⁻, and NH₄⁺ were important in the formation, nucleation, and growth of α -AgVO₃. These organizations based on symmetry can occur at three levels: short, medium, and long distances. Thus, the clusters can interact preferably, forming surfaces that can give rise to numerous morphologies (Figure 3). Because of the clusters, defects, and electronic density, complex clusters were formed with nonzero dipole moments. The dipole–dipole interactions may generate clusters with a defined number of atoms to favor growth in a particular direction. Thus, in complex clusters, there is a correlation among the electrons situated in the neighborhood of the [AgO₆] and [VO₄] complex clusters, provided by long-range interactions. This phenomenon harmonizes the interactions at short and medium ranges. Figure 3 indicates the formation of microrods of α -AgVO₃ crystals in the synthesis performed at 10 °C. These crystals showed defined faces and were elongated along the *y*-axis in the [110] direction. The diameters of the microrods were uniform throughout their lengths. At 20 °C, it can be seen that the microrods began to agglomerate, and some urchin-like microspheres were formed by the direct self-assembly of

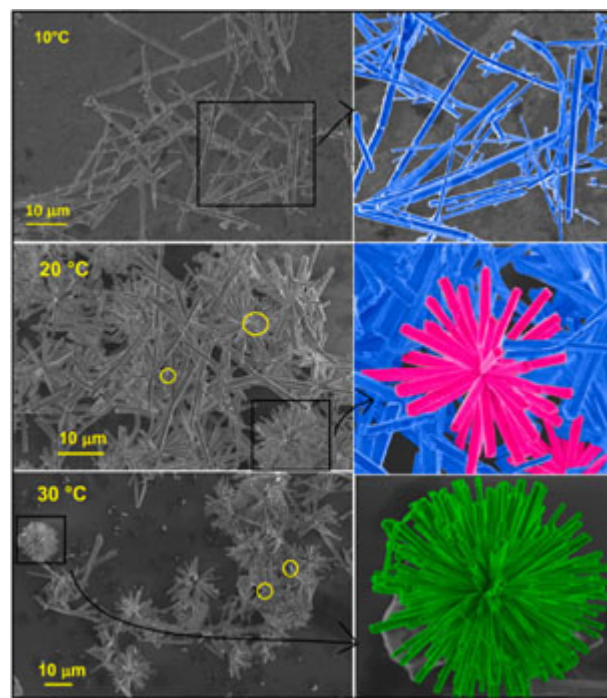


Figure 3. Field emission-SEM images of α -AgVO₃ powders obtained by the coprecipitation method at 10, 20, and 30 °C. Adapted from [7].

nanorods due to molecular interactions. At 30 °C, α -AgVO₃ crystals with urchin-like morphologies were predominantly formed.^[7]

Acetonitrile mediated the self-assembly of 1D nanowires into 3D spongy-like structures for enhanced performance of lithium ion batteries.^[31] The variation in the concentration of acetonitrile medium and the hydrothermal treatment transformed the nanowires into the β -AgVO₃ phase. Thus, acetonitrile played a major role in the growth of ultralong nanowires and self-assembly into 3D spongy-like structures.

Gonzales-Zavala et al. used a hybrid deposition configuration in which the film was formed by the interaction of a laser ablation plasma with a flux of atomic vapor.^[6] This was employed to prepare V₂O₅ thin films with different contents of silver. The structural characterization revealed that the materials formed after silver incorporation consisted of mixtures of V₂O₅, Ag₃VO₄ and AgVO₃ and that at high concentrations of Ag, the film consisted of AgVO₃ only. The surface morphology was also strongly affected by the Ag content, changing from a very smooth surface to nanobelts and finally nanoparticles forming the surface.^[6]

It has been reported a pure inorganic gel, AgVO₃, which does not present any carbon atoms and which forms irrespective of the counter ions of the precursor salts. It is presumed that in the gel there exists Ag...Ag interactions and a crucial arrangement of VO₃⁻ ions in the polymeric AgVO₃

unit which in turn induce a high capability to entrap a large volume of water within the interlaced fibrous network. The gel material extremely exhibits high sorption capacity which can be utilized in waste water treatment.^[37]

In addition, a mature technology on synthesis of silver vanadate is bionics, which nanotube clusters are synthesized through a dynamic template method mainly induced by the thermal perturbation nucleation effect and the template effect of polyacrylamide through the polymerization of acrylamide in the process of crystal growth.^[38]

4. Applications

4.1. Photocatalysis, Sensors and Tribology

Recent advancements in heterogeneous photocatalysis have focused on the design of visible-light responsive materials due to their potential application in hydrogen production from water splitting, degradation of organic pollutants and CO₂ reduction to high value hydrocarbon fuels.^[39–41] As a semiconductor, silver vanadate is one of the promising alternatives to enhance the photocatalytic ability, mainly because the optical absorption can be extended to the visible light region and effectively depress the recombination of the photo-generated electrons and holes, allowing the development of a feasible strategy to take full advantage of solar light at higher photocatalytic activity.^[42] This occurs because there are efficient absorption centers in the vanadate groups, VO₄³⁻, where electronic transitions can be easily induced from oxygen (2p orbital) to V⁵⁺ (3d orbital) ions.^[10] Many efforts have been made in the development of nanomaterials with photocatalytic activity under visible light irradiation for photodegradation of dyes or depletion of H₂O. The introduction of Ag⁺ ions into the lattices of vanadates originates from the strong hybridization between Ag-4d and O-2p orbitals, which induces narrowing of the band gap and lowering of the valence band energy of the semiconductors. The efficiency of solar conversion in photocatalysis is determined by optical absorption, hole-electron separation, hole-electron migration and recombination. The low energy-conversion efficiency in semiconductors is due to limitations in one or more of these four processes.^[43] According to reports, incorporation of Ag nanoparticles can enhance the efficiency of photovoltaic devices and improve the photocatalytic degradation of organic dyes. Ag nanoparticle incorporation can efficiently separate holes and electrons because metallic Ag has excellent conductivity and strong electron-trapping ability. Furthermore, Ag nanoparticles have surface plasmon resonance (SPR), which increases the optical absorption and electron-hole pair formation because of the electron-magnetic field near the surface.^[44] Excellent photocatalytic activity in dye photodegradation was confirmed

when silver vanadates were applied to rhodamine-B (RhB),^[9] methylene blue (MB)^[41] and industrial effluent.^[24]

During the last years, several Ag₂O/Ag₃VO₄/AgVO₃-GO,^[45] MoS₂/AgVO₃,^[46] InVO₄/AgVO₃,^[47] Ag/AgVO₃/RGO,^[48] AgVO₃/BiVO₄,^[49] AgVO₃/ZnFe₂O₄,^[50] g-C₃N₄/AgVO₃^[51] heterojunctions have been synthesized and exhibited excellent light-trapping ability and photocatalytic performance.

Silver vanadates also have semiconducting characteristics, and they can be applied as sensors. Mai et al. developed a AgVO₃ sensor for hydrogen sulfide (H₂S) detection.^[52] H₂S is one of the most toxic and odorous gases, which arises from the decomposition of organic compounds and industrial by-products. In this work, AgVO₃ nanowires were prepared by ultrasonic treatment and hydrothermal reaction with V₂O₅. This nanomaterial showed good H₂S sensing performance with short response, reaching low response concentrations of 50 ppm. Good H₂S selectivity was observed through little sensitivity toward H₂ and CO gas. The authors described that the detector exhibited a “threshold switching” phenomenon, where a high bias (i. e., 6 V) was required to switch the device from nonconductive to conductive. The response and recovery times were less than 10 s and 20 s, respectively.

High temperatures are the harshest conditions in tribology and are encountered in applications such as the aerospace, tooling and material forming, automotive, military and nuclear power industries. Transition metal oxides such as vanadium oxides are promising candidates as solid lubricant materials at elevated temperatures due to the possible formation of lubricious oxide phases. The silver vanadate nanorods showed good lubrication behavior at high temperature. This reduction in friction coefficient at high temperature can be associated with the evolution of a layered, low shearing, silver vanadate phase in combination with the segregation of silver at the surface.^[53,54]

4.2. Biomedical Applications

4.2.1. Silver Vanadium Oxides for Batteries

Vanadium has found innumerable applications in medicine, particularly because this element can mimic both enzymes for antioxidant activity^[55] and insulin.^[56] Xiang et al. demonstrated that AgVO₃ nanobelts (100 nm width and 0.5–5 μm length) presented peroxidase-like activity and could be used as a probe for quantitative determination of H₂O₂ (range from 0.075 to 0.5 mM).^[57] In terms of biomedical engineering, Bock et al. underlined the application of silver vanadium oxides for batteries in implantable cardiac defibrillators (ICD). Silver vanadium oxide enhances ICD devices, as it is a bimetallic cathode material with superior solubility, excellent electrical conductivity and minimized battery resistance. The

Table 3. Silver vanadate nanomaterials and their antibacterial activity.

Nanomaterial	Characteristics	Bacteria strains	Antibacterial activity	Ref.
AgVO ₃ nanowires	Nanowires: ~60 nm AgNPs: 1–20 nm	<i>S. aureus</i>	MIC = 3.4–12.5 µg mL ⁻¹	[19]
Silver vanadate nanorods	Diameter: 50–200 nm Length: 0.5–2 µm AgNPs: 20–30 nm	<i>P. aeruginosa</i> <i>E. coli</i> <i>S. aureus</i> <i>Lactobacillus fermentum</i>	MIC = 4 µg mL ⁻¹ MIC = 16–32 µg mL ⁻¹ MIC = 32–64 µg mL ⁻¹ MIC = 16–64 µg mL ⁻¹	[23]
AgVO ₃ nanorods	Diameter: ~80 nm Length: 3 µm	<i>E. coli</i> <i>B. subtilis</i>	MIC = 10 µg mL ⁻¹ MIC = 30 µg mL ⁻¹	[29]
Ag/AgVO ₃ nanowires	Morphologies: Nanorods Urchin like	<i>E. coli</i> <i>B. subtilis</i> <i>S. aureus</i>	MIC = 1 µg mL ⁻¹ MIC = 5 µg mL ⁻¹ MIC = MBC = 62.5–125 µg mL ⁻¹	[30]
Ag/VO _x nanotubes	Nanotubes: 20–75 nm [a]AgNPs: 3–10 nm	<i>E. coli</i> <i>S. aureus</i>	[b]MIC = 0.4 µg mL ⁻¹ MIC = 3.15 µg mL ⁻¹ [c]MBC = 3.15–6.25 µg mL ⁻¹	[64]
β-AgVO ₃ nanowires	Nanowires: 20–60 nm AgNPs: 5–40 nm	<i>S. enterica</i> Typhimurium <i>E. coli</i> <i>E. faecalis</i>	MIC = MBC = 3.15 µg mL ⁻¹ MIC = MBC = 1.0 µg mL ⁻¹ MIC = 5.0 µg mL ⁻¹ MBC > 69.0 µg mL ⁻¹	[65]
LiV ₂ O ₅ /Agnanocomposite	Diameter: 40–50 nm Length: 5–10 µm AgNPs: 2–10 nm	<i>B. subtilis</i> <i>E. coli</i> <i>P. aeruginosa</i>	MIC = 60 µg mL ⁻¹ MIC = 120 µg mL ⁻¹ Inhibition of Biofilm 83 % (6.25 µg mL ⁻¹) Bacterial inactivation	[66]
V ₂ O ₅ /AgNP nanofibers	Diameter: ~35 nm AgNPs: 5–65 nm	<i>S. aureus</i> <i>E. coli</i>	0.05 M 0.02 M	[67]

[a]AgNPs: Silver nanoparticles. [b]MIC: Minimal Inhibitory Concentration. [c]MBC: Minimal Bactericidal Concentration.

properties of silver vanadium oxide enabled the fabrication of ICD devices with low time required for recharge. The authors also highlighted the possibility of *in situ* formation of silver nanoparticles during the discharges, boosting the electrical conductivity of these batteries.^[58] New strategies for α-AgVO₃ and β-AgVO₃ 1D materials fabrication are of fundamental importance in the advancement of science and technology. These nanostructures have been demonstrated as promising cathode materials in lithium ion batteries.^[59,60] Nanocomposites have attracted increasing interest because 1D, 2D and 3D nanomaterials can offer a range of unique advantages in electrochemical and energy related fields.^[31,41,60–62] AgVO₃/polyaniline (PANI) triaxial nanowires^[63] improved the electrochemical performance of nanowire electrodes in Li ion batteries and as supercapacitors.

4.2.2. Nanostructured Silver Vanadium Oxides as Antimicrobial Agents

According to Li et al., nanostructures of vanadium hold advantages in the following aspects: the element is abundant,

and its synthesis is based on soft chemistry; their morphology provides access to different contact regions of the nanomaterial, which offer many possibilities for structural modification and functionalization; and its size and surface characteristics increase the reactive activity. In addition, the authors highlighted the possibility that the modification of vanadium oxide nanostructures with silver nanoparticles (AgNPs) could provide many interesting applications in electrochemistry, catalysis and biology.^[64] Particularly for biomedical applications, nanomaterials are promising to tackle the global concern regarding antibiotic resistance. The silver element is well known for its biocidal properties, and the most abundant literature on silver vanadium nanostructures for medicine is related to their enhanced antibacterial activity (Table 3).

Metallic nanomaterials such as vanadium and silver composites have the ability to physically interact with the surface of bacteria, and the nanoparticle shape, size and surface charge are somewhat important. However, the toxicity toward bacteria can be attributed to the release of toxic ions (particularly AgNPs that can be oxidized). The mechanisms

of toxicity to bacteria, production of reactive oxygen species, mainly by the Fenton reaction inside the cell, and membrane disruption are the main studied effects. Other mechanisms, such as protein dysfunction by oxidation of essential amino acids, impairment of enzyme activity (e.g., destruction of Fe–S clusters of enzymes) and interference in nutrient assimilation are described in the literature.^[68,69] In this manner, research on metal-based antimicrobial nanomaterials has now moved forward, and production of functional materials, such as coatings and antifouling paints of vanadium pentoxide nanoparticles,^[70] bactericidal water-based paints of silver vanadate nanocomposites^[66] and filtration membranes with embedded silver nanoparticles,^[71] has been reported. It is important to note that the elucidation of the health risks assessment of nanosilver vanadates must be cautiously evaluated for their proper use in biomedical applications. Furthermore, because β -AgVO₃ nanowires can reach the environment, ecotoxicological and biocompatibility studies are mandatory to their ecological risk assessment. In this way, our group reported the acute toxicity of AgVO₃ nanowires to *Daphnia similis*, an aquatic bioindicator, due to release of silver from the nanomaterial trapped in the organism.^[72]

4.2.3. Nanostructured Silver Vanadate for Dental Applications

The development of nanostructured silver vanadate decorated with AgNPs (β -AgVO₃) has emerged as a promising additive for acrylic resins to improve dentistry practice. This material has excellent antimicrobial property, as the silver and vanadium elements can act synergistically against the main pathogenic microorganisms found in the oral cavity.^[19] The application of this material avoids the agglomeration of nanoparticles, as it possesses a high dispersion of silver nanoparticles on silver vanadate nanowires, maintaining a larger surface contact with the microorganisms, and has a more suitable color for dental prostheses.^[19,65] The experimental design adopted so far by researchers to implement nanostructured resins for dental application involves an integrative and multidisciplinary approach. The synthesis of nanostructured silver vanadate (β -AgVO₃) is performed via a precipitation reaction between silver nitrate (AgNO₃) and ammonium metavanadate (NH₄VO₃) in an aqueous medium.^[19] The resulting β -AgVO₃ consists of nanowires with an average diameter of 150 nm and a length on the micrometer scale coated with 25-nm semispherical metallic silver particles (Figure 4a). The resins are then prepared by mixing different concentrations of β -AgVO₃ (ranging from 0% to 10%) with the desired mass of polymer acrylic resins commonly used in dental materials (Figure 4b and 4c). Finally, the impact of the incorporation of β -AgVO₃ on the antimicrobial (Figure 4d)

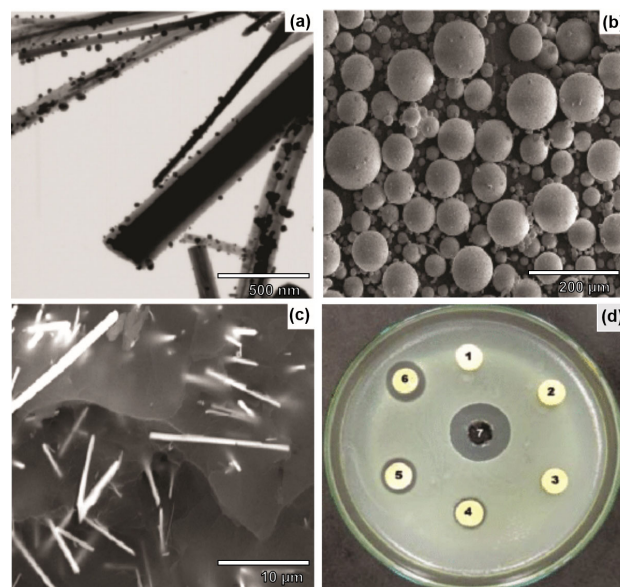


Figure 4. Scanning transmission electron microscopy image of β -AgVO₃ treated with AgNPs (a); scanning electron micrograph of the polymer used in the preparation of the resin (b) and fracture surface of thermopolymerizable containing 5% β -AgVO₃ (c); zone of inhibition formed with β -AgVO₃ against *Staphylococcus aureus* (ATCC 25923) (d). 1–0%; 2–0.5%; 3–1.0%; 4–2.5%; 5–5.0%; 6–10% and 7- solution of chlorhexidine gluconate at 0.05%. The Figure 4a, 4b–1c, and 4d were adapted from references [74], [75] and [73], respectively.

and mechanical properties of dental acrylic resins is evaluated.^[73–74]

Table 4 summarizes the studies regarding nanostructured silver vanadate acrylic resins for dental application. de Castro et al.^[73] were the first to explore the effects of the addition of silver vanadate nanowires decorated with AgNPs on the antimicrobial activity, surface hardness, and compressive strength of dental acrylic resin. They demonstrated that the incorporation of β -AgVO₃ has the potential to promote antimicrobial activity in the acrylic resin in a dose-dependent manner. The properties of dental resins were increased with the addition of reduced rates of β -AgVO₃, and at higher rates, no negative influence compared with the control was observed.^[72] The incorporation of AgVO₃ into different endodontic sealers and its antimicrobial activity, flow and radiopacity were also evaluated.^[74] The results showed that adding AgVO₃ may improve the antimicrobial effect of the endodontic sealers without major changes in their physico-chemical properties. Nevertheless, an in vitro study performed to evaluate the influence of the growth of pathogenic microorganisms on the surface of two acrylic resins incorporated with nanostructured silver vanadate and the impact strength revealed important clinical implications.^[63] The incorporation of β -AgVO₃ into acrylic resins may reduce the risk of opportunistic infections caused by the contamination

Table 4. Studies regarding nanostructured silver vanadate acrylic resins for dental application.

Nanomaterial ^[a]	Dental resin	Biological activity	Mechanical and/or physical properties	Reference
β -AgVO ₃ nano-wires	Self-curing Dencor Lay – Clássico [®]	<i>S. aureus</i> <i>S. mutans</i> <i>P. aeruginosa</i> <i>C. albicans</i>	Surface hardness Compressive strength	[72]
AgVO ₃ nano-wires	AH Plus (DENTSPLY DeTrey GmbH, Konstanz, Germany) Sealapex (Sybron Endo, Orange, CA, USA) Sealer 26 (DENTSPLY, Petropolis, Brazil) Endofill (DENTSPLY, Petropolis, Brazil)	<i>E. faecalis</i> <i>P. aeruginosa</i> <i>E. coli</i>	Flow Radiopacity	[73]
β -AgVO ₃ nano-wires	Autopolymerizing (AP) (Dêncor Lay; Clássico Dental Articles) Heatpolymerizing (HP) (Clássico; Clássico Dental Articles)	<i>P. aeruginosa</i> <i>S. aureus</i>	Impact strength	[74]
β -AgVO ₃ nano-wires	Dencor Lay autopolymerizable (SC) Clássico thermopolymerizable (TR) (Clássico Artigos Odontológicos [®])	<i>C. albicans</i> <i>S. mutans</i>	Flexural strength Hardness Surface roughness	[75]
AgVO ₃ nano-wires	Autopolymerising (AP) (Dêncor Lay; Clássico Dental Articles) Heatpolymerising (HP) (Clássico; Clássico Dental Articles)	Fibroblasts L929 cell	Measurement of metal ion release	[76]

^[a] The nanomaterial characteristics are described in the text.

of dental prostheses due to significant antibacterial activity; however, this material can increase the possibility of prosthesis fracture. In this sense, more efficient addition methods should be investigated to improve the dispersion pattern of β -AgVO₃ in the polymer matrix to prevent reduction in the impact strength of resins.^[75] The antibiofilm activity of two acrylic resins containing β -AgVO₃ against microorganisms associated with dental prostheses was investigated.^[8] The hardness, surface roughness, and flexural strength of the resins were also evaluated. These mechanical properties associated with antibiofilm action are factors directly related to the effectiveness of the material in the oral cavity. The addition of β -AgVO₃ to dental acrylic resins promoted antibiofilm activity and did not change the mechanical properties of hardness and surface roughness of the resins, although the flexural strength decreased with the addition of loads higher than 1%, indicating that the viability of clinical use should be evaluated in terms of changes in some of the mechanical properties.^[76] The methodological difficulty of dispersing β -AgVO₃ in resins suggests that the mixing procedures adopted were not efficient enough to disperse the resins evenly in the system. Furthermore, because β -AgVO₃ nanowires can be released into the environment, ecotoxicological and biocompatibility studies are mandatory to evaluate their environmental health and safe application. The release of Ag and V ions to determine how this release affected the cell viability of L929 fibroblasts.^[77] A positive correlation was found between the concentration of AgVO₃ and the ion release, and a negative

correlation was found between the ion release and the cell viability. Significant concentrations of Ag and V ions were released from resins with higher loads of AgVO₃. The leachates presented cytotoxicity for cells, suggesting that the use of low concentrations in resins is required to avoid risks to patients.

5. Patent Market of the Silver Vanadate

In the context of science related to silver vanadate-based materials, technological applications deserve special attention since the demand for the transformation of generated knowledge in the laboratory toward the development of novel products is growing worldwide. Figure 5 shows the evolution

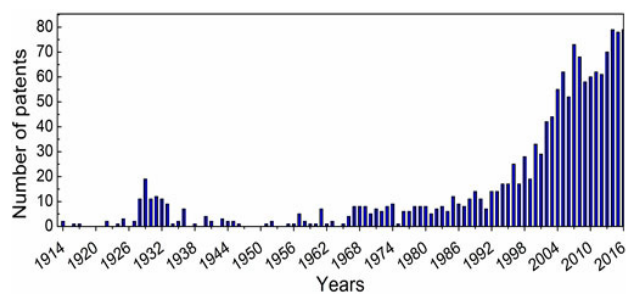


Figure 5. Number of worldwide published patents regarding silver vanadate based technologies.

in the number of patents for silver vanadate materials over time. The graph was elaborated through Questel Orbit advanced patent search program using the following keywords with their respective joint operators and wildcard characters: ((silver* 3D vanadat*) OR (nanosilver* 3D vanadat*) OR (silver* 3D nanovanadat*) OR (nanosilver* 3D nanovanadat*) OR (Ag 3D vanadat*) OR (nanoAg 5D vanadat*) OR (Ag 5D nanovanadat*) OR (nanoAg 5D nanovanadat*) OR Ag₃VO₄ OR AgVO₃ OR Ag₄V₂O₇), being found 626 results later used in the statistical analysis.

The interface between a research center and industry is the intellectual property management through patents, as they are related to technology transfer processes. Thus, market analysis linked to case studies of relevant patents on silver vanadate production and related products was carried out on this topic. The first patent was published on July 7, 1914, i.e., the American patent US1102670A.^[78] The document is related to the production process of sulfur acid anhydride from the reaction between sulfur dioxide and oxygen gases using an inorganic support based on silver vanadate as the catalyst agent.

The dissemination of scientific and technological knowledge related to the catalytic properties of silver vanadate materials can be traced back to the beginning of the 20th century. The patent AU2010294679 B2^[79] was filed in Australia on September 3, 2010 and subsequently granted by the Australian Patent Office (IP Australia). The patent comprises an aqueous antimicrobial dispersion in a hybrid network. The antimicrobial activity is related to the presence of silver vanadate salt embedded in a silica-acrylate copolymer-based inorganic matrix. This technology was proposed for antimicrobial applications and for coatings. The U.S. patent application US20120071671A1^[80] filed on March 22nd, 2012 at the United States Patent and Trademark Office (USPTO) comprises a multimetal catalyst agent containing silver vanadate as one of the active catalyst components. This technology, among several applications, was proposed for the oxidation of gaseous hydrocarbons such as toluene, o-xylene and p-xylene. In the abovementioned patents, silver vanadate holds a particular importance in its application as a catalyst agent.

Another interesting case study is related to the patent JP4676428 B2^[81] granted on April 27, 2011 by the Japanese Patent Office (JPO). One of the inventions contemplated in the document relates to an imaging device composed of electrode layers. The intermediate layer is composed of silver vanadate owing to its dielectric capacitor characteristics. By applying a potential difference between the electrodes, electrons are emitted at the upper electrode for imaging. This is an example of an electrochemical technological application of silver vanadate among several available related patents.

The patent US7754111 B1^[82] was granted by the United States Patent and Trademark Office (USPTO) on July 13, 2010. This document reports the production method of silver vanadium oxyfluoride for lithium electrochemical cells. In this process, silver vanadate is mixed with other raw materials, such as silver fluoride and vanadium oxytrifluoride, to obtain the final mentioned product. The interesting applications include the use of electrochemical cells (containing silver vanadate in the presence of fluoride) in medical equipment such as cardiac defibrillators, pacemakers, drug pumps and neurostimulators. The mentioned patent is an example of a semiconductor application of silver vanadate among several available related technologies.

6. Conclusions

The general concept of this paper is to provide an overview of techniques available for the synthesis of silver vanadate nanostructures and its physicochemical nature. This work also provides insight into the current technologies and applications involving this promising nanomaterial. It is important to note that there is a single synthesis technique recommended over other techniques, i.e., hydrothermal treatment, which has been used by the vast majority of research groups active in the area. Particular attention is given to the antibacterial, electrochemical and photocatalytic activities. The construction of specific nanostructured architectures with various dimensions, including zero-, one-, two-, and three-dimensional (0D, 1D, 2D, and 3D) nanomaterials, owing to their unique size- and/or shape-dependent physicochemical properties, is presented.

Therefore, considerable efforts will be made to fabricate AgVO₃ with different morphologies. With respect to the photocatalytic applications, there are already several successful demonstrations of the use of silver vanadate. For the case of electrochemical technological application of silver vanadate among several available related patents, silver vanadates are excellent candidates for the development of the so-called third generation electrochemical devices, and many promising reports can be found in the literature in this particular area. Regarding the antibacterial activity, nanosilver vanadates demonstrate high efficiency for a range of pathogenic bacteria, in crude form or incorporated into complex matrices. Despite the progress in many of these applications, further improvements in the synthesis and processing of silver vanadates are necessary to improve device functionality. Given the great promise offered by silver vanadates in its nanof orm, we can only predict that it will continuously attract more interest by the scientific community in the near future.

Acknowledgement

The authors thank the National Council for Technological and Scientific Development (CNPq), the Laboratory of Synthesis of Nanostructures and Interaction with Biosystems (NanoBioss), and the National Institute of Science Technology and Innovation in Complex Functional Materials (INOMAT/INCT) for the financial and general support.

References

- [1] K. J. Takeuchi, A. C. Marschilok, S. M. Davis, R. A. Leising, E. S. Takeuchi, *Coord. Chem. Rev.* **2001**, *219*, 283–310.
- [2] M. I. Bertoni, N. J. Kidner, T. O. Mason, T. A. Albrecht, E. M. Sorensen, K. R. Poeppelmeier, *J. Electroceram.* **2007**, *18*, 189–195.
- [3] M. S. Whittingham, *Chem. Rev.* **2004**, *104*, 4271–4301.
- [4] S. Kittaka, K. Matsuno, H. Akashi, *J. of Solid State Chem.* **1999**, *142*, 360–367.
- [5] P. Rozier, J. M. Savariault, J. Galy, *J. Solid State Chem.* **1996**, *122*, 303–308.
- [6] Gonzalez-Zavala, L. Escobar-Alarcon, D. A. Solis-Casados, C. Rivera-Rodriguez, R. Basurto, E. Haro-Poniatowski, *Appl. Phys. A* **2016**, *122*, 461–469.
- [7] R. C. de Oliveira, C. C. de Fogggi, M. M. Teixeira, M. D. P. da Silva, M. Assis, E. M. Francisco, B. N. A. D. Pimentel, P. F. D. Pereira, C. E. Vergani, A. L. Machado, J. Andres, L. Gracia, E. Longo, *ACS Applied Materials & Interfaces* **2017**, *9*, 11472–11481.
- [8] C. Wu, H. Zhu, J. Dai, W. Yan, J. Yang, Y. Tian, S. Wei, Y. Xie, *Adv. Funct. Mater.* **2010**, *20*, 3666–3672.
- [9] S. Bao, Q. Bao, C. Li, T. P. Chen, C. Sun, Z. Dong, Y. Gan, J. Zhang, *Small* **2007**, *3*, 1174–1177.
- [10] F. Cheng, J. Chen, *J. Mater. Chem.* **2011**, *21*, 9841–9848.
- [11] R. Konta, H. Kato, H. Kobayashi, A. Kudo, *Phys. Chem. Chem. Phys.* **2003**, *5*, 3061–3065.
- [12] D. P. Singh, R. M. Yadav, T. P. Yadav, *Rev. Adv. Sci. Eng.* **2012**, *1*, 319–340.
- [13] H. E. Roscoe, *J. Chem. Soc.* **1871**, *24*, 23–36.
- [14] M. A. Ditte, *Compt. rendus* **1887**, *104*, 1705–1708.
- [15] P. E. Browning, H. E. Palmer, *Amer. J. Sci.* **1910**, *30*, 220–222.
- [16] H. T. S. Britton, R. A. Robinson, *J. Chem. Soc. London* **1930**, 2328–2343.
- [17] H. T. S. Britton, R. A. Robinson, *J. Chem. Soc. London* **1933**, 512–517.
- [18] P. Fleury, R. Kohlmuller, M. G. Chaudron, *C. R. Acad. Sc. Paris* **1966**, *262*, 475–477.
- [19] S. Sharma, M. Panthoefler, M. Jansen, A. Ramanan, *Mat. Chem. And Physics* **2005**, *91*, 257–260.
- [20] R. D. Holtz, A. G. Souza, M. Brocchi, D. Martins, N. Duran, O. L. Alves, *Nanotechnology* **2010**, *21*.
- [21] C. Belver, C. Adán, S. García-Rodríguez, M. Fernández-García, *Chemical Engineering Journal* **2013**, *224*, 24–31.
- [22] T. Chen, M. Shao, H. Xu, C. Wen, S.-T. Lee, *Journal of Colloid and Interface Science* **2012**, *366*, 80–87.
- [23] J. Zhou, Q. Liang, A. Pan, X. Zhang, Q. Zhu, S. Liang, G. Cao, *J. Mater. Chem. A* **2014**, *2*, 11029–11034.
- [24] T. A. Vu, C. D. Dao, T. T. T. Hoang, P. T. Dang, H. T. K. Tran, K. T. Nguyen, G. H. Le, T. V. Nguyen, G. D. Lee, *Materials Letters* **2014**, *12*, 176–180.
- [25] V. Sivakumar, R. Suresh, K. Giribabu, V. Narayanan, *Solid State Sciences* **2015**, *39*, 34–39.
- [26] H. Li, H. Li, S. Wu, C. Liao, Z. Zhou, X. Liu, A. B. Djuri, M. Xie, C. Tang, K. Shih, *Journal of Alloys and Compounds* **2016**, *674*, 56–62.
- [27] L. Dong, G. Guan, X. Wei, X. Zhao, M. Xv, *Journal of Alloys and Compounds* **2016**, *677*, 12–17.
- [28] J. Xie, X. Cao, J. Li, H. Zhan, Y. Xia, Y. Zhou, *Ultrasonics Sonochemistry* **2005**, *12*, 289–293.
- [29] F. Mohandes, M. Salavati-Niasari, *Ultrasonics Sonochemistry* **2013**, *20*, 354–365.
- [30] A. Singh, D. P. Dutta, A. Ballal, A. K. Tyagi, M. H. Fulekar, *Materials Research Bulletin* **2014**, *51*, 447–454.
- [31] R. F. De Luis, A. Martinez-Amesti, E. S. Larrea, L. Lezama, A. T. Aguayo, M. I. Arriortua, *J. Mater. Chem. A* **2015**, *3*, 19996–20012.
- [32] W. Klockner, R. M. Yadav, J. Yao, S. Lei, A. Aliyan, J. Wu, A. A. Martí, R. Vajtai, P. M. Ajayan, J. C. Denardin, D. Serafini, F. Melo, D. P. Singh, *J Nanopart Res* **2017**, *19*, 288–301.
- [33] C. Wu, H. Zhu, J. Dai, W. Yan, J. Yang, Y. Tian, S. Wei, Y. Xie, *Adv. Funct. Mater.* **2010**, *20*, 3666–3672.
- [34] C. Han, Y. Pi, Q. An, L. Mai, J. Xie, X. Xu, L. Xu, Y. Zhao, C. Niu, A. M. Khan, X. He, *Nano Lett.* **2012**, *12*, 4668–4673.
- [35] P. Ju, H. Fan, B. Zhang, K. Shang, T. Liu, S. Ai, D. Zhang, *Separation and Purification Technology* **2013**, *109*, 107–110.
- [36] M. Feng, L.-B. Luo, B. Nie, S.-H. Yu, *Adv. Funct. Mater.* **2013**, *23*, 5116–5122.
- [37] S.-H. Jang, J. H. Yoon, Y.-D. Huh, S. Yoon, *J. Mater. Chem. C* **2014**, *2*, 4051.
- [38] C. Mondal, M. Ganguly, J. Pal, R. Sahoo, A. K. Sinha, T. Pal, *Chem. Commun.* **2013**, *49*, 9428–9430.
- [39] Xiao-Yu Yuan, Feng-Rui Wang, Jin-Ku Liu, Xiao-Hong Yang, *Crystal Growth & Design* **2017**, *17*, 4254–4264.
- [40] L. Yang, Y. Wan, Y. Huang, H. Weng, L. Qin, H. J. Seo, *J. Taiwan. Inst. Chem. Eng.* **2016**, *66*, 400–406.
- [41] S. Liang, X. Zhang, J. Zhou, J. Wu, G. Fang, Y. Tang, X. Tan, *Mater. Lett.* **2014**, *116*, 389–392.
- [42] S. Zhang, S. Peng, S. Liu, L. Ren, S. Wang, J. Fu, *Mater. Lett.* **2013**, *110*, 168–171.
- [43] Y. Lu, Y. Wan, S. Bi, H. Wen, Y. Huang, H. J. Seo, *Mater. Chem. Phys.* **2016**, *180*, 263–271.
- [44] X. Q. An, J. C. Yu, F. Wang, C. H. Li, *Appl. Catal., B: Environ* **2013**, *129*, 80–88.
- [45] S. Khanchandani, S. Kundu, A. Patra, A. K. Ganguli, *J. Phys. Chem. C* **2013**, *117*, 5558–5567.
- [46] R. Rana, X. Menga, Z. Zhan, *Applied Catalysis B: Environmental* **2016**, *196*, 1–15.
- [47] L. Cao, *Materials Letters* **2017**, *188*, 252–256.
- [48] Z. Xin, Z. Jie, Y. Jianqiang, Z. Yan, C. Zhaoxia, S. Yan, H. Baorong, *Applied Catalysis, B: Environmental* **2018**, *220*, 57–66.

- [48] W. Zhao, J. Li, Z. Wei, S. Wang, H. He, C. Sun, S. Yang, *Applied Catalysis B: Environmental* **2015**, *179*, 9–20.
- [49] R. Wang, L. Cao, *Journal of Alloys and Compounds* **2017**, *722*, 445–451.
- [50] R. Abazari, A. R. Mahjoub, *Industrial & Engineering Chemistry Research* **2017**, *56*, 623–634.
- [51] X. Lin, D. Xu, S. Jiang, F. Xie, M. Song, H. Zhai, L. Zhao, G. Che, L. Chang, *Catalysis Communications* **2017**, *89*, 96–99.
- [52] L. Mai, L. Xu, Q. Gao, C. Han, B. Hu, Y. Pi, *Nano. Lett.* **2010**, *10*, 2604–2608.
- [53] S. M. Aouadi, D. P. Singh, D. S. Stone, K. Polychronopoulou, F. Nahif, C. Rebholz, C. Muratore, A. A. Voevodin, *Acta Materialia* **2010**, *58*, 5326–5331.
- [54] P. Singh, K. Polychronopoulou, C. Rebholz, S. M. Aouadi, *Nanotechnology* **2010**, *21*, 325601–325608.
- [55] A. A. Vernekar, D. Sinha, S. Srivastava, P. U. Paramasivam, P. D'Silva, G. Muges, *Nat Commun* **2014**, *5*.
- [56] Z. J. Guo, P. J. Sadler, *Angewandte Chemie-International Edition* **1999**, *38*, 1513–1531.
- [57] Z. B. Xiang, Y. Wang, P. Ju, D. Zhang, *Microchimica Acta* **2016**, *183*, 457–463.
- [58] D. C. Bock, A. C. Marschilok, K. J. Takeuchi, E. S. Takeuchi, *Journal of Power Sources* **2013**, *231*, 219–225.
- [59] H. Zeng, Q. Wang, Y. Rao, *RSC Advances* **2015**, *5*, 3011–3015.
- [60] L. Sun, Y. Zhang, J. Li, T. Yi, X. Yang, *Chemistry of Materials* **2016**, *28*, 4815–4820.
- [61] L. Liang, Y. Xu, Y. Lei, H. Liu, *Nanoscale* **2014**, *6*, 3536–3539.
- [62] L. Mai, X. Xu, C. Han, Y. Luo, L. Xu, Y. A. Wu, Y. Zhao, *Nano. Lett.* **2011**, *11*, 4992–4996.
- [63] R. S. Diggikar, M. V. Kulkarni, G. M. Kale, B. B. Kale, *J. Mater. Chem. A* **2013**, *1*, 3992–4001.
- [64] J. Li, L. F. Zheng, K. F. Zhang, X. Q. Feng, Z. X. Su, J. T. Ma, *Materials Research Bulletin* **2008**, *43*, 2810–2817.
- [65] R. D. Holtz, B. A. Lima, A. G. Souza, M. Brocchi, O. L. Alves, *Nanomedicine-Nanotechnology Biology and Medicine* **2012**, *8*, 935–940.
- [66] R. S. Diggikar, R. H. Patil, S. B. Kale, D. K. Thombre, W. N. Gade, M. V. Kulkarni, B. B. Kale, *Applied Microbiology and Biotechnology* **2013**, *97*, 8283–8290.
- [67] S. Poyraz, I. Cerkez, T. S. Huang, Z. Liu, L. T. Kang, J. J. Luo, X. Y. Zhang, *Acs Applied Materials & Interfaces* **2014**, *6*, 20025–20034.
- [68] J. A. Lemire, J. J. Harrison, R. J. Turner, *Nature Reviews Microbiology* **2013**, *11*, 371–384.
- [69] J. R. Morones-Ramirez, J. A. Winkler, C. S. Spina, J. J. Collins, *Science Translational Medicine* **2013**, *5*.
- [70] F. Natalio, R. Andre, A. F. Hartog, B. Stoll, K. P. Jochum, R. Wever, W. Tremel, *Nature Nanotechnology* **2012**, *7*, 530–535.
- [71] A. F. de Faria, A. C. M. de Moraes, P. F. Andrade, D. S. da Silva, M. do Carmo Gonçalves, O. L. Alves, *Cellulose* **2017**, *24*, 781–796.
- [72] M. C. Artal, R. D. Holtz, F. Kummrow, O. L. Alves, G. A. Umbuzeiro, *Environ. Toxicol. Chem.* **2013**, *32*, 908–912.
- [73] D. T. de Castro, R. D. Holtz, O. L. Alves, E. Watanabe, M. L. Valente, C. H. da Silva, *J. Appl. Oral. Sci.* **2014**, *22*, 442–449.
- [74] A. B. V. Teixeira, C. L. Vidal, D. T. de Castro, C. de Oliviera-Santos, M. A. Schiavon, A. C. dos Reis, *Eur. Endod. J.* **2017**, *2*, 16.
- [75] D. T. de Castro, M. L. Valente, J. A. Agnelli, C. H. Lovato da Silva, E. Watanabe, R. L. Siqueira, O. L. Alves, R. D. Holtz, A. C. dos Reis, *J. Prosthet. Dent.* **2016**, *115*, 238–246.
- [76] D. T. de Castro, M. L. Valente, C. H. da Silva, E. Watanabe, R. L. Siqueira, M. A. Schiavon, O. L. Alves, A. C. Dos Reis, *Arch. Oral Biol.* **2016**, *16*, 46–53.
- [77] D. T. Castro, M. L. D. C. Valente, C. P. Aires, O. L. Alves, A. C. dos Reis, *Gerodontology* **2017**, *34*, 320–325.
- [78] H. V. Keler, A. Weindel, Patent US1102670A, **1914**.
- [79] C. C. Peng, M. Ramanujachary, A. Fechtenkotter, S. Thevigha, M. Huang, F. Faugeroux, S. Chee, B. D. Mehta, *Patent AU2010294679 B2*, **2011**.
- [80] A. K. Mannheim, H. H. Schriesheim, C. D. Mannheim, C. K. D. Ludwigshafen, F. R. Mannheim, N. B. M. Rettigheim, S. S. H. Rohrbach *Patent US20120071671A*, **2012**.
- [81] S. Kazuto, A. Saburo, H. Koji, N. Nobuyaso, N. Tomonari, Y. Takamase, *Patent JP4676428 B2*, **2011**.
- [82] J. W. Williamsville, E. S. T. E. Amherst, R. L. Williamsville, *Patent US7754111 B1*, **2010**.

Received: October 5, 2017

Accepted: December 22, 2017

Published online on January 11, 2018